The Generic Design of a High-Traffic Advanced Metering Infrastructure Using ZigBee

Hoi Yan Tung, Kim Fung Tsang, *Member, IEEE*, Kwok Tai Chui, Hoi Ching Tung, Hao Ran Chi, Gerhard P. Hancke, *Senior Member, IEEE*, and Kim Fung Man, *Fellow, IEEE*

***Abstract*—A multi-interface ZigBee building area network (MIZBAN) for a high-traffic advanced metering infrastructure (AMI) for high-rise buildings was developed. This supports meter management functions such as Demand Response for smart grid applications. To cater for the high-traffic communication in these building area networks (BANs), a multi-interface management framework was defined and designed to coordinate the operation between multiple interfaces based on a newly defined tree-based mesh (T-Mesh) ZigBee topology, which supports both mesh and tree routing in a single network. To evaluate MIZBAN, an experiment was set up in a five-floor building. Based on the measured data, simulations were performed to extend the analysis to a 23-floor building. These revealed that MIZBAN yields an improvement in application-layer latency of the backbone and the floor network by 75% and 67%, respectively. This paper provides the design engineer with seven recommendations for a generic MIZBAN design, which will fulfill the requirement for demand response by the U.S. government, i.e. a latency of less than 0.25 s.**

***Index Terms*—Advanced Metering Infrastructure (AMI), building area network (BAN), multi-interface, smart grid, ZigBee.**

I. Introduction

ADVANCED metering infrastructure (AMI) is an important milestone of smart grid development [1]–[4]. Different smart-grid communication technologies and standards have been introduced [2]. Apart from smart metering, AMI also facilitates utilities to perform demand response, and thus energy demand is reduced [5]–[7]. Therefore, various AMI pilot projects have been implemented around the world, e.g. in Australia, Japan, the United States, and Europe, and most of these are designed for individual homes.

Recent trials of AMI in Asian countries involved high rises in which signal penetration is much more difficult because of the typical hard reinforced concrete structure in such buildings. Moreover, the large amount of electric meters scattered in high rises drives the need to accommodate high data flow which supersedes ordinary slower data flow AMI in the U.S. or Europe, where normally data will be sent back to a utility from a single house. Such a huge aggregation of data creates the need to investigate building area networks (BANs) to cater for high-traffic AMI (HTAMI) [8]–[10]. A successful BAN requires good connectivity.

A wireless sensor network is a potential candidate for BAN, and it has been widely adopted in industrial automation which transmitted the data over large areas using its multi-hopping ability [11]. ZigBee is one of the well-known wireless sensor network standards, and it has been widely adopted in different AMI projects as a result of its intrinsic mesh property, which provides good scalability and connectivity. In addition, the wireless characteristics facilitate a "plug and play" behavior which benefits retrofitting into existing premises. As a matter of fact, in May 2009, ZigBee was recognized by the USA government as an open standard for the smart grid [12]. In light of the development of BAN, a generic architecture of ZigBee BAN (ZBAN) is proposed in this paper. The proposed ZBAN may be easily, accurately, and efficiently deployed in high-density-traffic BANs, such as in high rises.

Based on the discussion of a ZBAN design for HTAMI, this paper set up a role model for BAN, which handles the inter-floor and infra-floor communication separately by using the Backbone Network (BN) and Floor Network (FN), respectively. As a result, BN and FN can adopt different designs in order to cater for their own traffic characteristics. For example, a multi-interface design has been proposed for the BN of ZBAN, while a single interface design has been adopted for the FN. It is because the traffic loading of BN is much heavier than FN. The design of BN and FN is not limited to ZigBee development but can apply any communication media, including wire line and wireless technology.

To support the multi-interface BN development of ZBAN a multi-interface management framework (MIMF) was defined and designed such that it coordinates the operation between multiple interfaces, rendering the DR latency requirement [13] ulfilled. It is important to highlight that the development of MIMF is not the original intention of this paper. However, the revious work of dynamic channel management algorithms fo- used on the single interface device [14], [15] which did not handle the adjacent channel interference from multi-interfaces, and, thus, they cannot be applied in this case. Even though some multi-interface WiFi designs have been discussed recently [15], [16], these designs cannot be directly adopted to ZBAN because the network characteristics of ZigBee and WiFi are the same. WiFi is a star network while ZigBee is a mesh network. Owing to these reasons, MIMF has been in development for the BN development of ZBAN.

H. Y. Tung, K. F. Tsang, K. T. Chui, H. R. Chi, and K. F. Man are with the Department of Electronic Engineering, City University of Hong Kong, Kowloon, Hong Kong (e-mail: hytung@cityu.edu.hk; ee330015@cityu.edu.hk; ktchui3-c@my.cityu.edu.hk; haoranchi2-c@my.cityu.edu.hk; eekman@cityu.edu.hk).

H. C. Tung is with the School of Engineering, City University, London EC1V 0HB, U.K. (e-mail: cherry.tung.1@cityu.ac.uk).

G. P. Hancke is with the University of Pretoria, Pretoria 0002, South Africa (e-mail: g.hancke@ieee.org).

The novelty in the MIMF design is twofold. First, MIMF minimizes the impact of adjacent channel interference by proposing a brand-new channel-selection mechanism for network formation. Second, a transmission interface-selection algorithm has been defined on top of the ZigBee route-selection procedure to ensure the device always transmits with the best condition interface and balancing the traffic load between different interfaces. By adopting the standard tree address assignment, MIMF supports a newly designed tree-based mesh (T-Mesh) network which provides both tree and mesh routing to maximize routing strength. Such a T-Mesh design is the first of its kind.

The detailed design of the MIMF will be discussed in later sections. We will explain that the developed multi-interface ZBAN (MIZBAN) can be efficiently adopted in high-traffic BANs (e.g., high rises) to facilitate demand side management (DSM), which in turn improves the electricity generation efficiency.

This paper is organized as follows. The design of ZBAN for HTAMI is discussed in Section II. The development of MIMF for HTAMI is presented in Section III, and a real-world application of an AMI solution is described in Section IV. The performance evaluation of MIZBAN is given in Section V. Finally, a conclusion is given in Section VI.

II. High Traffic ZigBee BAN for HTAMI

ZigBee belongs to the class of wireless sensor networks whose adoption bears a crucial meaning. It was discussed that, because of the inherent nature of scalability and mesh capability of ZigBee, ZBAN for AMI can be established and set up quickly in most existing buildings at a lower cost. Such an adaptive and scalable wireless structure will certainly help to build up an efficient demand response smart metering infrastructure for various smart grid applications. A good demand and response smart metering system will help the gross domestic product (GDP) grow healthily (less carbon emission) to a great extent.

Attention should be drawn to the fact that traffics in a BN in a high-rise BAN is a few hundred times more than in a traditional AMI network used for individual houses or low rises. Since data are normally collected every 15–30 min, the major challenge presented to the AMI system in a high-rise BAN is the design of high density traffic for smart metering.

From the HTAMI system design perspective, high-density meter data aggregation in the backbone yields high traffic. In addition, it is not uncommon that wireless local area networks (WLANs) are normally used in households. WLANs operate in the same frequency band as ZigBee at 2.4 GHz. Under such circumstances, closely packed packets of different standards around the same general area may cause inference to the target AMI system. However, it was well documented that ZigBee and WiFi may coexist [18]. Hitherto, the remaining issue is to design a mechanism for high traffic. To tackle the challenge of high traffic, the network structure of a multi-interface ZigBee BAN (MIZBAN) is proposed, and its conceptual architecture is illustrated in Fig. 1.

MIZBAN is divided into two parts: the multi-interface backbone, in short, BN (vertical), and the single-interface mesh floor network, in short, MFN (horizontal). Each interface represents a frequency channel.

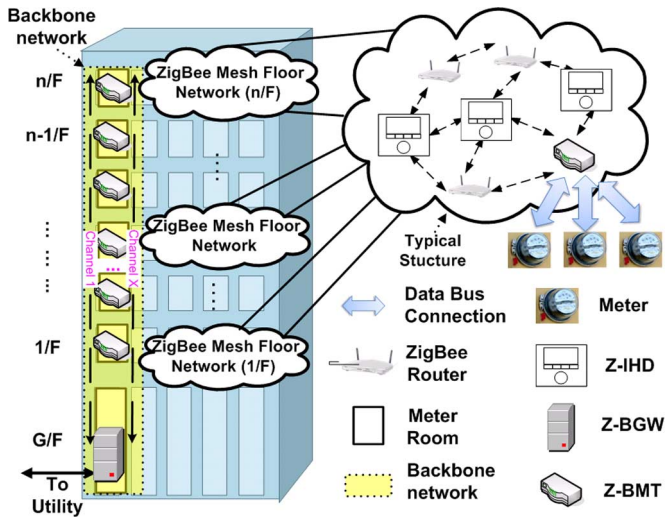

Fig. 1. MIZBAN design for HTAMI.

The MFN is discussed first. It consists of two basic components: in-home displays (Z-IHD) and ZBAN meter terminals (Z-BMT). Referring to Fig. 1, Z-IHD and Z-BMT belong to an MFN (horizontal) and are located at different premises on each floor. The Z-BMT is the interception point of the MFN and the BN. It connects to multiple electric meters using data buses, since electric meters are normally centralized into the meter room. If the Z-IHDs/Z-BMTs are situated at locations where the coverage cannot be reached by the MFN, a ZigBee router is added to relay the message to target devices. Z-IHDs, Z-BMTs and ZigBee routers are configured to form a ZigBee mesh network that can be easily established in each premise on a floor. The timely energy consumption and the price rate information can be delivered to users at any time when a user presses a button on the Z-IHD.

On the other hand, the BN consists of many Z-BMTs and a ZBAN Gateway (Z-BGW). A Z-BMT on a floor deals with horizontal traffic as well as vertical traffic. While the horizontal traffic allows energy audit and profiling, the vertical traffic facilitates a batch-mode data aggregation, thus rendering DSM. It is thus seen that a Z-BMT embraces traffic for both the MFN and the BN.

The BN (vertical) is now discussed. It consists of two basic components: Z-BMT and Z-BGW. The incorporation of these units furnishes the features of load profiling and meter management. In the BN, meter readings are collected from the electric meters via a Z-BMT located on the corresponding floor. Meter data are aggregated (wirelessly) from Z-BMT to Z-BMT until they finally reach the Z-BGW. The Z-BGW is a unique device in a BAN that aggregates energy data from Z-BMT and transmits the data to the backend server of the utility.

The most challenging mission of MIZBAN is that the BN must ensure that the data flow between Z-BMTs in a BAN bear sufficient signal strength and the signal transmission be accomplished with reasonably low latency. Based on the demand, a multi-interface framework accommodating multiple channels is developed. To facilitate fast data delivery (and thus low latency), a ZigBee MIMF was devised in the MIZBAN BN. The

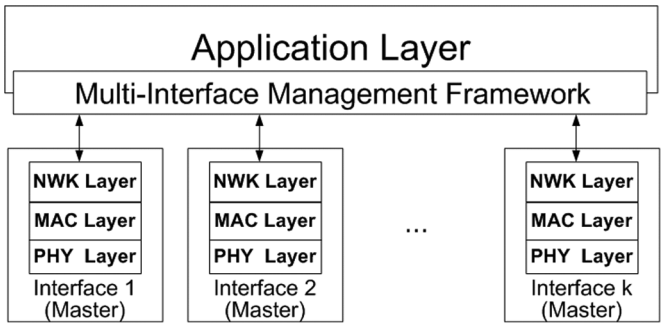

Fig. 2. Multi-interface ZigBee architecture.

vision is to enable parallel transmission by using multiple interfaces. Thus, the transmission time will decrease dramatically as the number of parallel channels is increased. However, parallel channels may incur potential adjacent interference.

To combat potential interference, MIZBAN has further enhanced the ZigBee mesh capability by providing more redundancy paths under different interfaces to minimize latency. It should be recapitulated that the novelty in this new design is that the developed MIMF considers the LQI in the entire transmission path instead of the traditional localized LQI. Thus, the MIMF facilitates the MIZBAN the minimum routing cost with high throughput, low latency, and low interference.

As an illustration, consider the case for a dual-interface BN, where a Z-BMT on the sixth floor sends the collected meter data to the Z-BGW on two radio interfaces A and B under channels 1 and 2, respectively. Suppose channel 1 (interface A) suffers from the interference (from any source causing communication failure) originating from the third floor. Once the sender detects that the transmission fails, the data are sent to the Z-BGW via channel 2 (interface B). Since multi-interface is the essential technology of the MIZBAN backbone, the design of ZigBee MIMF will be discussed in detail in Section III.

III. Multi-Interface Management Framework

It was explained in Section II that a MIMF is required to speed up the traffic by enabling parallel transmission with multiple interfaces in a MIZBAN BN. The MIMF is an application management module to coordinate the operation of different interfaces for the initialization of network formation and data transmission. It is vital to stress that the MIMF is an application module that may be implemented on top of any ZigBee protocol core, thus it is interoperable with new and old versions of the ZigBee standard. As a result, MIMF inherits MAC and network-layer characteristics of ZIgBee including routing, address assignment, and media access control. The proposed MIMF is a service sublayer that interacts with the application profile and multiple network layers. By taking these factors into consideration, a MIMF design incorporating the Z-BGW and the Z-BMT was introduced to support the backbone communication of MIZBAN. Since MIMF is created for HTAMI, a smart metering device is powered by the main supply in order to support a low-latency and high-reliability service. Therefore, energy efficiency is not the main concern for the MIMF design. The MIMF architecture for the management of ZigBee devices is shown in Fig. 2.

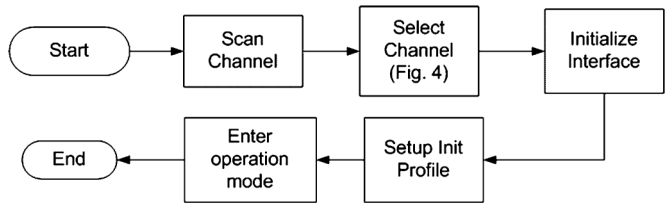

Fig. 3. Network formation procedure of multi-interface coordinator.

It is well documented that ZigBee devices are classified into coordinators, routers, and end devices. These devices play different roles in the network. The design of a network layer, a MAC layer, and a physical layer for individual interfaces should comply with IEEE 802.15.4 instead of IEEE 802.15.4e because IEEE 802.15.4e only supports the beacon-enabled mode without mesh routing capability. Based on the same reason, the beacon-enabled MAC scheduler designs [14], [19], [20] are not suitable for BAN development.

ZigBee supports both tree and mesh routing, as does MIMF. Outstanding from ZigBee, MIMF considers tree routing as a backup path of mesh routing. When mesh routing fails (for instance, as a consequence of routing table overflows), MIMF simply forwards the message to its parent (next hop of tree route which is defined by address assignment). The parent node can further handle message with mesh routing. Under such a curriculum, the service would not be suspended, and transmission delay would slightly increase. Such a novel design will be referred to hereafter as T-Mesh.

In the present design of the MIMF for MIZBAN, the Z-BGW is configured as the coordinator and the Z-BMT is configured as the router. Thus, the Z-BGW takes care of the network formation and mitigates potential interference. In essence, the Z-BGW initializes a personal area network (PAN) and governs the router discovery and provides permission for members joining the PAN. The Z-BGW and the Z-BMT will determine the best transmission interface to achieve a low latency which renders an efficient DSM.

A. Network Formation

In brief, the network formation procedure of the MIMF ZigBee Coordinator (Fig. 3) is similar to the formation of an ordinary ZigBee network. First, the coordinator performs the channel scanning via the master interface in order to acquire the LQI of the channel. LQI, similar to the ordinary meaning of receive signal strength indicator (RSSI), is defined in the ZigBee standard as a measure of the channel signal strength. After the channel scanning is performed, the coordinator selects the operating channel for each interface. To minimize the adjacent channel interference and ensure the channel quality, a channel selection algorithm was developed. The algorithm is shown in Fig. 4.

After every interface has been initialized, the coordinator enters the operation states and other ZigBee devices such as routers and end devices may join the network. On the other hand, the multi-interface router, which is a unique device, also performs channel scan with its master interface. The master interface of the router initializes with the best LQI channel and joins the multi-interface network. The router then receives

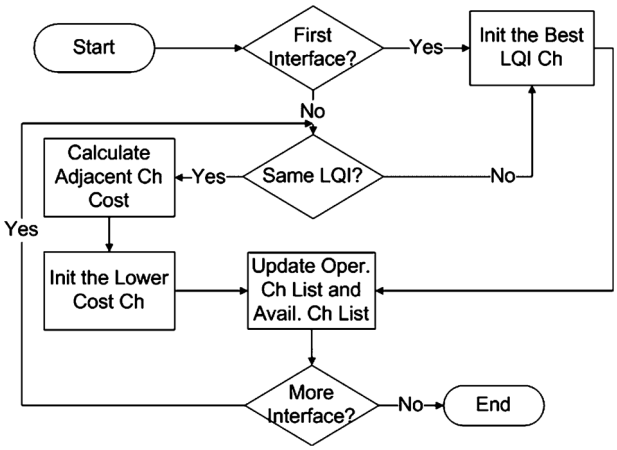

Fig. 4. Channel selection algorithm.

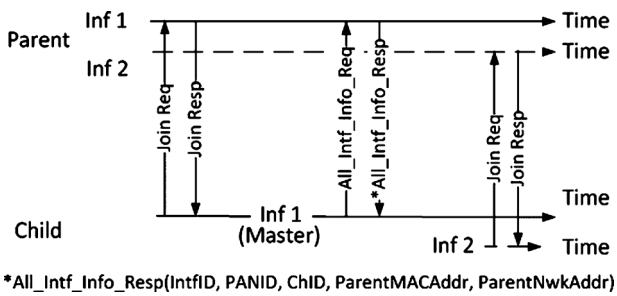

Fig. 5. Initialization process for a multi-interface router.

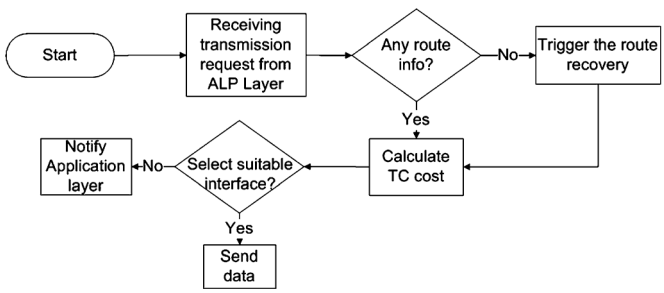

Fig. 6. Transmission interface selection algorithm for MIMF.

an all-operation channel ID from the master interface, and, subsequently, the router initializes the rest of the interfaces with given channel IDs. The initialization process of a ZigBee router is summarized in Fig. 5.

B. Data Transmission

To further enhance the network performance, the MIMF devices select the interface with the lowest transmission cost for data transmission. The interface selection algorithm is applied to both the coordinator and routers. The details of the data transmission are illustrated in Fig. 6.

After receiving the data transmission request, MIMF checks its route database which records the transmission cost of every interface for a specific destination. If MIMF does not find any record in the database, it instructs all interfaces to initiate a ZigBee standard route discovery to record path cost ($C\{P\}$) and round-trip time (RTT). RTT generally defines the period of time from sending out data/request to receiving the corresponding acknowledgment/response. Path cost indicates the link quality of routing path, and it is defined by ZigBee standard [21]. With end to end routing path information, the transmission cost (TC) of every interface can be calculated. For interface i, the transmission cost (TC_i) is given as

$$\mathrm{TC}_i = \mathrm{RTT}_i \times C\{P\}_i. \tag{1}$$

Certainly, the lowest transmission cost interface will be selected and the selection result will also be recorded in the route database. Typically, the transmission will be updated after every transmission have been completed because the new RTT can be recorded. Adoption of RTT has several advantages. Firstly, the RTT measurement is only carried by sender and so no extra network traffic has been generated. Second, RTT provides the updated transmission condition of the entire path because the path cost cannot be updated frequently because it can only be updated by performing route discovery, which may degrade the network performance. Furthermore, RTT can also indicate the workload of every interface because a long RTT may imply a high queuing delay. Therefore, it is a good indicator for load balance to avoid overloading a single interface.

Apart from RTT, path cost ($C\{P\}$) is another parameter for interface selection. Before going into details of path cost, the concepts of path and link must be introduced. A path P of length L refers to a routing path with $L-1$ hops which consists of L devices $[D_1, D_2\ \ldots\ D_L]$. A link l refers to a subpath of P between any two devices (a single hop) $[D_i, D_{i+1}]$. The link cost $C\{l\}$ for a link between device $[D_i, D_{i+1}]$ is a function with values in the interval $[0 \ldots 7]$ defined as [21]

$$C_i\{l\} = \min\left(7, round\left(\frac{1}{p_l^4}\right)\right) \tag{2}$$

where p_l is defined as the probability of packet delivery on the link l. According to the ZigBee standard [21], p_l is given as an average over the per-frame LQI value provided by the MAC layer and the maximum value of link cost is seven. With definition of link cost, the path cost $C\{P\}$ of a path P of length L is given as

$$C\{P\} = \sum_{i=1}^{L-1} C_i\{l\}. \tag{3}$$

IV. Real-World Application

A pilot was conducted in an existing residential high rise for the design and investigation of the performance of MIZBAN. As shown in Fig. 7, the building has 23 floors and each floor hosts ten electric meters. Such a building structure is recognized as a typical representative example of residential buildings in Hong Kong [22].

Since it is difficult to obtain measured data for the entire building, a minimum and yet sufficient amount of measured results using best effort was collected. Based on the measured data, a simulation model was developed to predict the network performance of the whole building. As a result, the case study is divided into two parts: experimental on-site testing (referred to as "Exp") and simulation evaluation (referred to as "Sim").

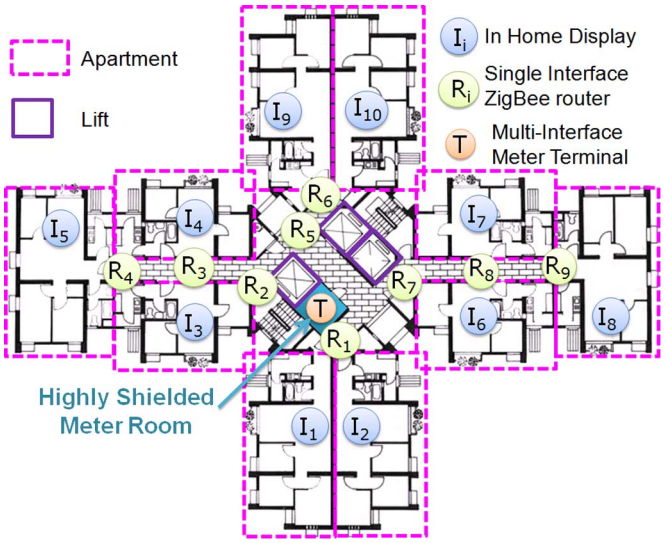

Fig. 7. ZigBee mesh floor network.

TABLE I
SYSTEM SPECIFICATION OF EXPERIMENTAL MIZBAN

Description	Given value
Number of floor, n	23
Number of apartment per floor, N_a	10
Number of record stored by smart meter, N_r	10
Record length, N_b, (bits)	32
AES 128bit enabled Payload length, L_p, (Bytes)	60
Packet length, L, (Bytes)	127
Transmission Power Pt	92mW
Receiver Antenna Gain Ar	0dBi
Transmitter Antenna Gain At	0dBi

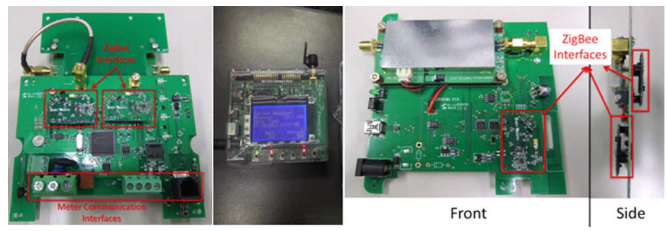

Fig. 8. Prototype of dual-interface MIZBAN. (a) Z-BMT. (b) Z-IHD. (c) Z-BGW.

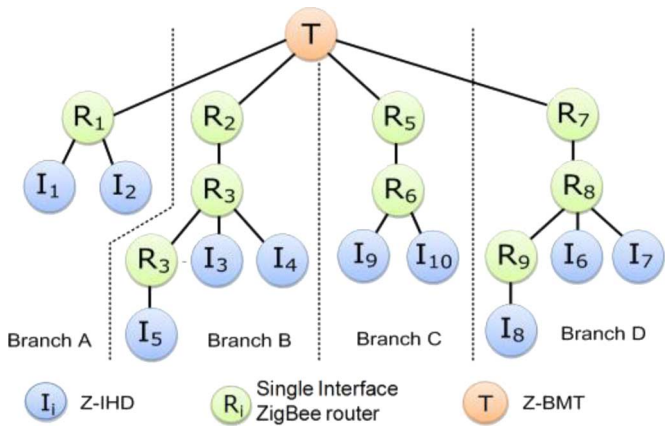

Fig. 9. ZigBee floor network tree.

A small-scale MIZBAN was set up to obtain the baseline data of the system performance. This is referred as minimum effort. The baseline data includes the FN tree and the signal propagation path. The FN tree and the signal propagation distance is a logical term determined by the transmitter power and the sensitivity of the receiver. Once these baseline parameters are determined, the model can be extended for a larger scale through simulation. An example will be given to illustrate this principle.

Based on key baseline data from experimental results, a simulation OPNET model was developed to project the MIZBAN performance for the entire building (23 floors). OPNET is an accurate model widely adopted by researchers for predictions [23]. An attenuation factor model [24] has been used in the simulation mode under configuration of baseline data was obtained from onsite testing. Thus the OPNET simulation describes the behavior of network performance from physical layer to network layer.

In the design, multi-interface ZigBee devices were implemented to operate with alternate channels. In order to minimize the interference, the channel numbers were separated by three in the design of [25], [26]. For instance, when the first interface occupies channel #1, then the second interface may use channel #5, and the third channel may use channel #9. Since there are only 16 channels in the 2.4-GHz ISM band, the multi-interface device could not support more than four interfaces. The experimental MIZBAN system specifications are summarized in Table I.

The experimental work is now presented. An experiment on MIZBAN consisting of five floors was performed (Fig. 1, $n = 5$). Since there were ten apartments per floor for five floors, the following devices were used for measurement: five dual-interface (dual-frequency channels) Z-BMTs, one dual-interface Z-BGW, ten single-interface ZigBee routers, and ten single-interface IHDs. The devices are shown in Fig. 8.

Implementation: The network was designed as a T-Mesh network. For implementation and valuation purposes, the ZigBee network was configured such that the five-floor BN and a FN (i.e., $n = 1$, e.g., the FN on the 5th floor, refer to Fig. 7) formed a single ZigBee mesh network. The signal propagation distance and FN tree were then determined.

For signal propagation distance, the maximum power was 100 mW in general (92 mW in the experiment) and the sensitivity -105 dBm, thus giving a dynamic range of >120 dB. Such a dynamic range normally allows a distance of propagation of about 80–100 m indoor and 1 km outdoor. Once the hop distance (or dynamic range) was determined, the number of routers could be determined. From the trial, it was determined that nine single-interface ZigBee routers $(R_1 - R_9)$ were needed to retain a quality transmission. As a result, the following system devices were used: the FN consisted of ten Z-IHDs $(I_1 - I_{10})$, nine single-interface ZigBee routers $(R_1 - R_9)$, and one dual-interface Z-BMT. The ZigBee FN tree shown in Fig. 9 was thus obtained and was used for simulation for network projection and evaluation of performance of the entire building.

It should be noted that the network in Fig. 9 refers to the address assignment. The network is not used for routing for most of situations nor does it form a tree network. The salient feature

TABLE II
INTERFACE ARCHITECTURE AND CAPACITY OF SCENARIOS 1–4

	Interface 1	Interface 2	Interface 3	Interface 4
Scenario 1, k=1 (Exp)	Branch A-D I_1-I_{10}, R_1-R_9 ($I_{c,1}$ = 19)	Nil	Nil	Nil
Scenario 2, k=2 (Exp)	Branch A-B I_1-I_5, R_1-R_4 ($I_{c,1}$ = 9)	Branch C-D I_6-I_{10}, R_5-R_9, ($I_{c,2}$ = 10)	Nil	Nil
Scenario 3, k=3 (Sim)	Branch A-B I_1-I_5, R_1-R_4 ($I_{c,1}$ = 9)	Branch C I_9-I_{10}, R_5-R_6 ($I_{c,2}$ = 4)	Branch D I_6-I_8, R_7-R_9 ($I_{c,3}$ = 6)	Nil
Scenario 4, k=4 (Sim)	Branch A I_3-I_5, R_2-R_4 ($I_{c,1}$ = 6)	Branch B I_9-I_{10}, R_5-R_6 ($I_{c,2}$ = 4)	Branch C I_6-I_8, R_7-R_9 ($I_{c,3}$ = 6)	Branch D I_1-I_2, R_1 ($I_{c,4}$ = 3)

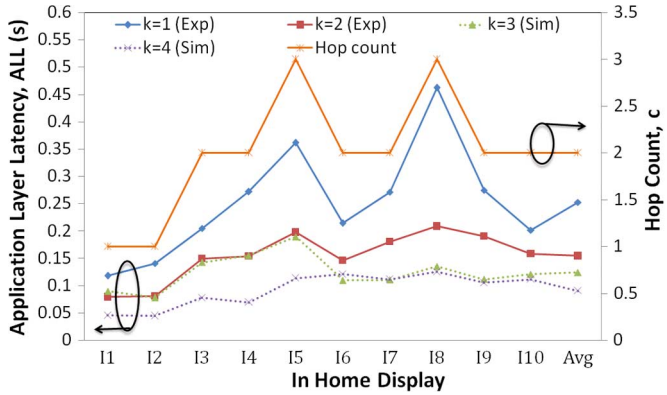

Fig. 10. ALL and c of $I_1 - I_{10}$ for k = 1–4 and n = 1.

of such a T-Mesh network is that when the mesh routing fails (e.g., routing table overflows), the tree routing will take the lead to route (as alternative route), thus enhancing the routing capability to a much greater extent. As a result, the mesh network and the tree routing form a complementary relationship to aid routing. The T-Mesh concept of implementation is the first of its kind in such investigation and measurement revealed that it is efficient.

Attention is now drawn to the impact on the number of interfaces (k). It was concluded in an earlier context that a maximum of four interfaces can be accommodated. As a result, four scenarios were designed. The configuration of the FN is summarized in Table II. Define $I_{c,i}$ as the capacity (which identifies the number of devices, including routers and IHDs, attached to a specific interface i of Z-BMT), and hop count c as the number of routers between the source and the destination. As an illustrative example, $I_{c,1} = 19$ for $k = 1$ (from Table II) indicates that there are 19 devices (including ten IHDs: $I_1 - I_{10}$ and nine ZigBee routers: $R_1 - R_9$) attached to interface 1 of Z-BMT. The scenarios to be investigated with details of interface architecture and capacity $(I_{c,i})$ are summarized in Table II.

To investigate user experience in real case, application-layer latency (ALL) and service level are recorded during the experiment. ALL refers to the duration from sending out a request to receiving a meter reading. To avoid handling time synchronization, ALL is chosen instead of other communication latency parameters such as end-to-end delay or jitter, because ALL is measured by the service requestor internally. For both floor network and backbone network testing, the service requestor requests the meter reading for every 15 min to meet the AMI requirement. Five hundred records were monitored (typically five days' work) in order to provide reliable basis data and smooth out irregularities due to potential inference and other possible factors like temperature and humidity variations. Service level refers to the response rate to a service request, and the service levels of all scenarios have been recorded as 100%. Therefore, the performance evaluation thereafter will mainly focus on ALL.

V. PERFORMANCE EVALUATION

The performance evaluation is divided into two parts: ZigBee mesh floor (horizontal communication) network and BN (vertical communication).

A. ZigBee Mesh Floor (Horizontal Communication) Network

Here, we investigate the latency experienced by an end user for a real-time meter reading request. A floor network has been set up as shown in Fig. 7. Ten Z-IHDs were configured as the service requestor while Z-BMT is the service responder. The average ALLs obtained from 500 experiment results ($k = 1$ and $k = 2$) and 500 simulation results ($k = 3$ and $k = 4$) are summarized in Fig. 10. Also, the hop counts (c) from Z-BMT to I_1 to I_{10} are given in Fig. 10.

Fig. 10 gives ALL and c between Z-IHDs $(I_1 - I_{10})$ and Z-BMT for $k = 1$–4 and $n = 1$. In general, ALL is directly proportional to c and declines as k increases. Among $I_1 - I_{10}$, the values of c for I_5 and I_8 (i.e., $c = 3$) are the highest and thus their ALLs are also ranked top two in all scenarios. The discrepancy of ALL I_5 and I_8 is given by the random back off period (T_b) during the media access which is also known as media access delay (d). Owing to the geographical location, the routing paths from Z-BMT to $I_1 - I_{10}$ remain unchanged when k increases from 1 to 4 and hence the values of c for $I_1 - I_{10}$ remain constant throughout scenarios 1–4.

It is important to highlight that the decline of ALL is not caused by diminishing c but rather due to the decrease of I_c. When $I_{c,i}$ decreases, d also decreases because MIZBAN has adopted carrier sense multiple access with collision avoidance (CSMA/CA) for media access control. The CSMA/CA mechanism avoids collision by sensing the media before transmission. If the sender finds that the channel is busy, it will wait for a period of T_b before sensing the channel again. Data transmissions are carried out only if the channel is idle after T_b. Otherwise, the device will wait for another T_b. Now define d as the delay of the entire media access process. As $I_{c,i}$ decreases, the probability of a channel busy drops and results in a decrease of d as well as ALL. Hence, ALL decreases as k increases.

Observing from Fig. 10, the average ALL is 0.25 s when $k = 1$ and $I_{c,1} = 19$ while the average ALL is improved by 40% (0.15 s) for $k = 2$ because $I_{c,i}$ is only one half of scenario 1. Comparing with scenario 2, the improvement of scenario 3 is minor because only $I_6 - I_{10}$ (5 IHDs) benefit from increasing k. With the same reason, only the ALL of $I_1 - I_5$ is improved in scenario 4 when compared to scenario 3.

Finally, the average ALL of scenario 4 $(k = 4)$ is 0.09 s which has been enhanced by 64%. Attention is drawn to the

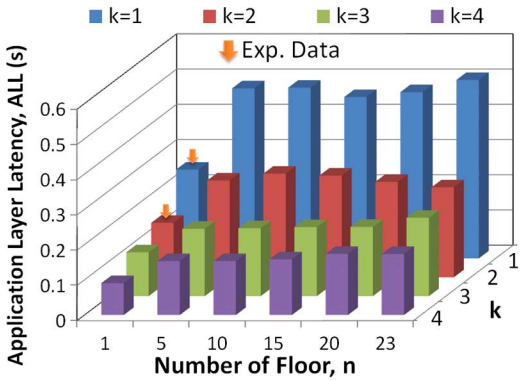

Fig. 11. ALL of ten IHDs (I1–I10) when k = 1–4 and n = 1–23.

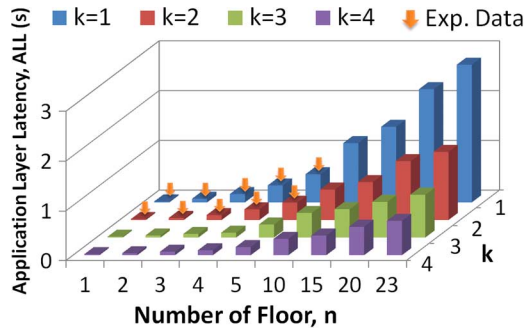

Fig. 12. Average ALL of $\mathrm{M_{k,n}}$ where k = 1–4 and n = 1–23.

fact that the discussion up to this point only focuses on the case of a single FN (n = 1). To investigate the FN performance under a multi-storey building, a simulation was conducted using OPNET and the ALL is shown in Fig. 11.

Fig. 11 illustrates the relationship between the height of the building (in terms of the number of floor, n) and average ALL of $\mathrm{I_1 - I_{10}}$ when k = 1–4. Regardless of n, the average ALL decreases as k increases, hence benefiting high-traffic situations. From Fig. 11, the average ALL is 0.51 s when k = 1 and it drops to 0.17 s (improved by 67%) as k increases to 4. In the mean time, $\mathrm{I_{c,}}_i$ drops from 19 to 3–6 which is only 15%–30% of $\mathrm{I_{c,}}_i$ for k = 1. Owing to the same reason, the experimental ALL is improved by 40% dropping from 0.25 to 0.15 s when k increases from 1 to 2. From Fig. 11, average ALL increases dramatically when n increases from 1 to 5. This phenomenon can be explained by using an example.

When ZigBee devices including routers, Z-IHDs and Z-BMT on the nth floor, detect the signal from other devices on the $(n-1)$th and $(n+1)$th floor, these ZigBee devices will be attached to the same interface and thus $\mathrm{I_{c,}}_i$ becomes three times $n = 1$. In addition, d also increases because there is higher probability to find a busy channel. However, the average ALL for n = 5–23 remains at a similar value because the measured ZigBee signal strength typically only penetrates between two floors. In essence, it was determined that the coverage entailed three floors but without good LQI to ensure quality reception. In such a case, parallel data transmission can be performed. Therefore, the discrepancy of average ALL for n = 5–23 is very small and, as a matter of fact, simulation revealed that the difference is only a random factor of $\mathrm{T_b}$.

It is important to highlight that MIZBAN provides real time meter reading to end users with the average latency bounded by 0.5 s for the 23-floor residential building under investigation. Therefore, it is concluded that the floor mesh network of MIZBAN supports dedicated services to end users for high-traffic communication in high rises.

B. Backbone Network (Vertical Communication)

Here, the performance of the MIZBAN BN is investigated. To reflect the real situation and understand the impact of the height of the building (the density of traffic), five BNs were established for n = 1–5. The testing network consisted of one to five dual interface Z-BMTs, $\mathrm{M_{k,n}}$, where k is the number of interfaces used in the experiment (i.e., k = 1–2) and n indicates the height of the building in terms of the number of floor (i.e., n = 1–5), and dual-interface Z-BGW (located in the meter room of ground floor, see Fig. 1).

The Z-BGW performs meter reading collection 500 times and so the average ALLs have been recorded for each testing networks (n = 1–5). Later, these experimental results were compared with the average ALL 500 simulation results for k = 3–4 in order to study the impact of the number of interfaces (k) on the BN performance of MIZBAN. Apart from the investigation of k = 3–4, the simulation model also predicted the performance of the BN for n = 10, 15, 20, and 23. The experimental and simulated results are plotted in Fig. 12.

Fig. 12 illustrates the average ALL of $\mathrm{M_{k,n}}$ where k = 1–4 and n = 1–23. In general, the average ALL decreases as k increases. With a constant number of electric meters, the traffic loading is shared among different interfaces as k increases and hence there is a higher probability of finding an idle channel. As a result, $\mathrm{T_b}$ as well as d will decrease.

On the other hand, the average ALL is found to be directly proportional to the height of the building since c (hop count between Z-BGW and Z-BMT) increases as the height increases. As a result, the average ALL increases. Furthermore, the improvement of ALL is more obvious as n increases because the traffic load of MIZBAN increases due to the number of served apartment increasing. Finally, it is important to pinpoint that the average ALL of the entire test building (n = 23) is reduced from 2.8 to 0.7 s (improved by 75%) by increasing k from 1 to 4.

It is also vital to highlight that MIZBAN does not only cater for the Smart Metering (SM) but also demand response (DR). Typically, the latency requirement of SM is from 2 to 15 s while DR is from 0.5 s to several minutes [13]. Now focusing on MIZBAN, the above latency requirements is further categorized into the backhaul latency (referring to the time taken from utility to Z-BGW) and the BAN latency (referring to the time taken from Z-BGW to Z-IHD). It is concluded that the BAN latency should not be more than 50% of the entire latency requirement. Therefore, the tightest latency requirement for MIZBAN is 0.25 s. To fulfill this requirement, the following recommendations are proposed for MIZBAN design.

1) Every Z-BGW should not serve more than 150 energy meters and the maximum hop count of the backbone network should be limited to no more than fourteen.

2) Z-BGW should NOT be located at the meter room of the ground floor in order to maximize the number of served floors. For example, Z-BGW should locate at the meter room of the 15th floor if the maximum hop count is 14 and the ZigBee signal can only propagate a single floor. Under these assumptions, a Z-BGW can serve 30 floors.
3) A single-interface MIZBAN is recommended for a building with no more than 40 energy meters and at the same time no more than three hops for the backbone network.
4) A tri-interface MIZBAN is recommended for a building with 41–90 energy meters and with a maximum hop count of the backbone network no more than eight.
5) A quadra-interface ZigBee device is recommended for a building with more than 90 energy meters and no more than 14 hops for the backbone network;
6) A Z-IHD and a ZigBee router that are within coverage but located on different floors should be attached to different interfaces.
7) A Z-IHD should be connected to the MIZBAN meter terminal by not more than three hops in the coverage.

By adopting the above recommendations and based on the results from Fig. 10 and Fig. 12, the BAN latency is estimated to be 0.245 s, i.e., $(0.09 + 0.4)/2$. Certainly, more than MIZBAN can be set up in a building if the hop count limit is exceeded. Without considering the latency requirement, the limitation of MIZBAN is inherited from the ZigBee standard which only supports 6500 devices in a single network and it is believed that can cover most buildings. Even though a multi-interface has been adopted, the transmission speed is relatively low comparing to other wireless technology such as WiFi. However, such limitation is outweighed by the mesh capability of ZigBee. The major advantage of MIZBAN is that it is aligned with the Zigbee standard, which has been adopted in a wide range of home automation systems and also commonly used by the smart meter. Therefore, MIZBAN can be further applied in different demand side management applications in any high rise building with a meter room. By incorporating the proposed MIMF, the MIZBAN has been successfully developed. Real-time measurement shows that the MIZBAN efficiently supports real-time smart-grid applications.

VI. Conclusion

To facilitate efficient deployment of AMI for existing buildings, a first BAN is presented in this paper which suggested breaking the network into backbone and floor network to handle inter-floor and infra-floor communication separately.

To gain more insight, this paper discussed the practical design of a BAN based on ZigBee. To cater to high traffic and meet the U.S. government latency requirement, a MIMF was defined and designed to coordinate the operation between multiple interfaces based on a newly designed T-Mesh ZigBee. As a result, a ZigBee MIZBAN is proposed for HTAMI.

A pilot was conducted. By conducting an experiment and using a simulation model, the ALL of the backbone network and the floor network was investigated. From the experimental results, it has been proved that the performance of the backbone and floor network improved by 40% if the number of network interface increases from one to two. By adopting the quadric-interface ZigBee module in a measurement in a twenty-three floor building, the AMI improved the ALL of the backbone and the mesh floor network by 75% (at 0.7 s) and 67% (at 0.09 s) respectively. To help designers to design HTAMI, this paper has made seven recommendations for MIZBAN (refer to Section V). Such recommendations ensure the design of AMI to fulfill the tightest US government Demand Response requirement for a latency value of less than 0.25 s.

There are two directions for future work. First, the BAN design will further applied to other communication media including wire line and wireless in order to conduct a comparative study. As a result, the full picture of the HTAMI development and recommendations can be provided. Second, the performance of MIZBAN will further be improved by conducting a coexistence study with other wireless technologies in order to strengthen its anti-interference capability.

Acknowledgment

The authors would like to thank Citycom Technology Ltd. and the Centre for Smart Energy Conversion and Utilization Research of City University of Hong Kong for providing the testing sites and testing facilities.

References

[1] A. Ipakchi and F. Albuyeh, "Grid of the future," *IEEE Power Energy Mag.*, vol. 7, no. 2, pp. 52–62, Mar.–Apr. 2009.
[2] V. C. Gungor, D. Sahin, T. Kocak, S. Ergut, C. Buccella, C. Cecati, and G. P. Hancke, "Smart grid technologies: Communication technologies and standards," *IEEE Trans. Ind. Inf.*, vol. 7, no. 4, pp. 529–539, Nov. 2011.
[3] P. Siano, C. Cecati, H. Yu, and J. Kolbusz, "Real time operation of smart grids via FCN networks and optimal power flow," *IEEE Trans. Ind. Inf.*, vol. 8, no. 4, pp. 944–952, Nov. 2012.
[4] W. Su, H. Eichi, W. Zeng, and M. Y. Chow, "A survey on the electrification of transportation in a smart grid environment," *IEEE Trans. Ind. Inf.*, vol. 8, no. 1, pp. 1–10, Feb. 2012.
[5] F. Benzi, N. Anglani, E. Bassi, and L. Frosini, "Electricity smart meters interfacing the households," *IEEE Trans. Ind. Electron.*, vol. 58, no. 10, pp. 4487–4494, Oct. 2011.
[6] J. Haase, J. M. Molina, and D. Dietrich, "Power-aware system design of wireless sensor networks: Power estimation and power profiling strategies," *IEEE Trans. Ind. Inf.*, vol. 7, no. 4, pp. 601–613, Nov. 2011.
[7] P. Palensky and D. Dietrich, "Demand side management: Demand response, intelligent energy systems, smart loads," *IEEE Trans. Ind. Inf.*, vol. 7, no. 3, pp. 381–388, Aug. 2011.
[8] Y. H. Jeon, "QoS requirements for the smart grid communications system," *Int. J. Comput. Inf. Sci.*, vol. 11, no. 3, pp. 86–94, 2011.
[9] Y. Simmhan, Q. Zhou, and V. K. Prasanna, "Chapter: Semantic information integration for smart grid applications," in *Green IT: Technologies and Applications*. Berlin, Germany: Springer, 2011.
[10] Z. M. Fadlullah, M. M. Fouda, N. Kato, A. Takeuchi, N. Iwasaki, and Y. Nozaki, "Toward intelligent machine-to-machine communications in smart grid," *IEEE Commun. Mag.*, vol. 49, no. 4, pp. 60–65, Apr. 2011.
[11] P. T. A. Quang and D. S. Kim, "Enhancing real-time delivery of gradient routing for industrial wireless sensor networks," *IEEE Trans. Ind. Inf.*, vol. 8, no. 1, pp. 61–68, Feb. 2012.
[12] U.S. DOE, "Locke, Chu Announce Significant Steps in Smart Grid Development," 2009. [Online]. Available: http://www.energy.gov/news2009/7408.htm.
[13] Dept. Energy Commun., "Communications requirements of smart grid technologies," Oct. 5, 2010.
[14] E. Toscano and L. L. Bello, "Multichannel superframe scheduling for IEEE 802.15.4 industrial wireless sensor networks," *IEEE Trans. Ind. Inf.*, vol. 8, no. 2, pp. 337–350, May 2012.
[15] Q. Yu, J. M. Chen, Y.-F. Fan, X.-M. Shen, and Y.-X. Sun, "Multichannel assignment in wireless sensor networks: A game theoretic approach," in *Proc. INFOCOM*, Mar. 2010, pp. 1–9.

[16] I. Ho, P. Lam, P. Chong, and S. Liew, "Harnessing the high bandwidth of multi-radio multi-channel 802.11n mesh networks," *IEEE Trans. Mobile Comp.*, vol. PP, no. 99, 2013, DOI: 10.1109/TMC.2013.9.
[17] D. J. Yang, X. Fang, and G. L. Xue, "Channel allocation in non-cooperative multi-radio multi-channel wireless networks," in *Proc. IEEE INFOCOM*, Mar. 2012, pp. 882–890.
[18] Y. Peizhong, A. Iwayemi, and Z. Chi, "Developing ZigBee deployment guideline under WiFi interference for smart grid applications," *IEEE Trans. Smart Grid*, vol. 2, no. 1, pp. 110–120, Mar. 2011.
[19] Z. Hanzálek and P. Jurčík, "Energy efficient scheduling for cluster-tree wireless sensor networks with time-bounded data flows: Application to IEEE 802.15.4/ZigBee," *IEEE Trans. Ind. Informat.*, vol. 6, no. 3, pp. 438–450, Aug. 2010.
[20] C. Caione, D. Brunelli, and L. Benini, "Distributed compressive sampling for lifetime optimization in dense wireless sensor networks," *IEEE Trans. Ind. Inf.*, vol. 8, no. 1, pp. 30–40, Feb. 2012.
[21] "ZigBee-2007 Specification," ZigBee Alliance, ZigBee Doc. 053474r17, Jan. 17, 2008.
[22] T. Y. Chen, J. Burnett, and C. K. Chau, "Analysis of embodied energy use in the residential building of Hong Kong," *Energy*, vol. 26, no. 4, pp. 323–40, Apr. 2001.
[23] OPNET University Program [Online]. Available: http://www.opnet.com/services/university/
[24] S. Y. Seidel and T. S. Rappaport, "914 MHz path loss prediction models for indoor wireless communications in multifloored buildings," *IEEE Trans. Antennas Propag.*, vol. 40, no. 2, pp. 207–217, Feb. 1992.
[25] E. Toscano and L. Lo Bello, "Cross-channel interference in IEEE 802.15.4 networks," in *Proc. WFCS*, May 2008, pp. 139–148.
[26] L. Lo Bello and E. Toscano, "Coexistence issues of multiple co-located IEEE 802.15.4/ZigBee networks running on adjacent radio channels in industrial environments," *IEEE Trans. Ind. Inf.*, vol. 5, no. 2, pp. 157–167, May 2009.

Hoi Yan Tung received the B.Eng. degree in information engineering (with First Class Honors) and Ph.D. degree from the City University of Hong Kong.

Currently, she is with Centre for Smart Energy Conversion and Utilization Research and the Department of Electronic Engineering, City University of Hong Kong. Her research interests are in wireless sensor network, energy management, and smart-grid communications.

Kim Fung Tsang (M'95) received the Ph.D. degree from the University of Wales, College of Cardiff, Cardiff, Wales.

During 1983–1988, he was a Research Assistant and a Product Executive. In March 1988, he joined the City University of Hong Kong, where he is now an Associate Professor with the Department of Electronic Engineering. His current research interests include radio-frequency circuit design, mobile communication network design, energy management, and wireless automation protocol design.

Kwok Tai Chui received the B.Eng. degree in electronic and communication engineering (with first-class honor) from City University of Hong Kong in 2013, where he is currently working toward the Ph.D. degree.

His research interest includes wireless communication, pattern recognition, health analysis, and machine learning algorithms.

Hoi Ching Tung received the B.Eng. degree in information engineering from the City University of Hong Kong in 2010. She is currently working toward the Ph.D. degree at the City University, London, U.K.

Her research interests are in wireless sensor network, energy consumption, and generation prediction.

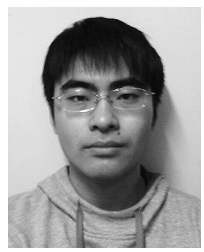

Hao Ran Chi received the B.Eng. degree in electronic and communication engineering (with first-class honors) from City University of Hong Kong in 2013.

Currently, he is a Research Assistant with the Department of Electronic Engineering, City University of Hong Kong. His research interests include artificial intelligence, electric vehicle battery management, and RF circuit design.

Gerhard P. Hancke (M'88–SM'00) received the B.Sc., B.Eng., and M.Eng. degrees from the University of Stellenbosch and the D.Eng. degree from the University of Pretoria, Pretoria, South Africa, in 1983.

He is a Professor and Coordinator of the Computer Engineering with the University of Pretoria, Pretoria, South Africa, and has played a major role in developing this program. He founded and is the Head of the Advanced Sensor Networks Research Group and is collaborating in research projects internationally. He has authored or coauthored more than 150 papers in peer-reviewed journals and international conference proceedings. His research interests are primarily in advanced industrial wireless sensor and actuator networks.

Kim Fung Man (M'91–SM'98–F'08) received the Ph.D. degree from Cranfield Institute of Technology, Cranfield, U.K.

He is a Chair Professor and Head of the Electronic Engineering Department at City University of Hong Kong. His research focuses on evolutionary computation, antenna and RF devices optimization, and control engineering. He has coauthored three books and published extensively in these area.

Prof. Man is currently the Co-Editor-in-Chief of the IEEE TRANSACTIONS OF INDUSTRIAL INFORMATICS.